

Dislocation charges reveal two-dimensional topological crystalline invariants

Guido van Miert¹ and Carmine Ortix^{1,2}

¹*Institute for Theoretical Physics, Centre for Extreme Matter and Emergent Phenomena, Utrecht University, Princetonplein 5, 3584 CC Utrecht, The Netherlands*
²*Dipartimento di Fisica “E. R. Caianiello”, Università di Salerno, IT-84084 Fisciano, Italy*

We identify a one-to-one correspondence between the charge localized around a dislocation characterized by a generic Burgers vector and the Berry phase associated with the electronic Bloch waves of two-dimensional crystalline insulators. Using this correspondence, we reveal a link between dislocation charges and the topological invariants of inversion and rotation symmetry-protected topological insulating phases both in the absence and in the presence of time-reversal symmetry. Our findings demonstrate that dislocation charges can be used as generic probes of crystalline topologies.

Introduction – The majority of topological phases of matter are characterized by anomalous surface states, whose presence or absence is linked to a topological index [1, 2]. The Chern number classifying quantum Hall insulators, for instance, counts the number of chiral states appearing at an isolated edge [3–5]. Their anomaly clearly resides in the fact that it is impossible to have a one-dimensional (1D) crystal with a different number of right-moving and left-moving electronic channels. For topological phases protected by additional (non)spatial symmetries, surface states are anomalous since they do not fulfil the minimal requirements of the protecting symmetry. Time-reversal symmetry, for instance, dictates that in a 1D system of spin one-half fermions, the Fermi energy E_F must always intersect an even number of Kramers’ pairs, a condition that is clearly violated by the helical edge states of two-dimensional quantum spin-Hall insulators [6–9]. The Dirac cones appearing in three-dimensional topological (crystalline) insulators are yet another example of these surface state anomalies [10–18]. The resolution of the paradox is simple: the Dirac cones, chiral or helical edge state appearing at the opposite edge always regularize the system and cancel the anomaly. However, revealing the anomaly of the electronic states at isolated surfaces with local probes gives immediate access to the topological invariant of the system [19–23].

There exists other topological states of matter, which are *not* characterized by anomalous surface states. This holds, in particular, for topological crystalline invariants associated to spatial symmetries that interchange the edge or surfaces of the system. In two-dimensional crystals with inversion symmetry, for instance, one can define two \mathbb{Z}_2 topological invariants corresponding to the quotients of the parities of the Bloch waves at $M = (\pi, \pi)$ and $X_1 = (\pi, 0)$ and M and $X_2 = (0, \pi)$, respectively. Signatures of this crystalline topology can be linked to peculiar properties of both the entanglement spectrum [24], and the electronic contribution to the charge polarization [25, 26]. But the presence of anomalous edge states mandated by topology is not guaranteed in these crystals.

Moreover, the peculiar properties of the entanglement

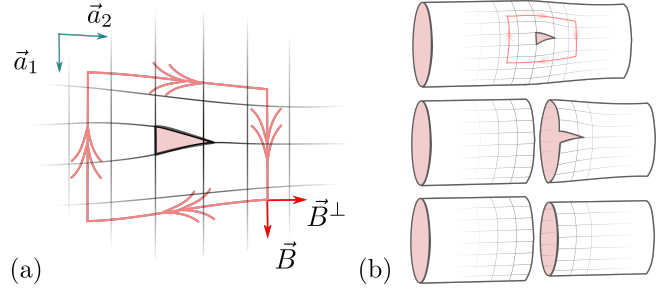


FIG. 1: (a) Schematic close-up of an edge dislocation. (b) Formation of a dislocation by gluing two cylinders. We find $\vec{B} = \vec{a}_1$, and $\vec{B}^\perp = \vec{b}_2 / (2\pi \|\vec{a}_1 \times \vec{a}_2\|)$. Here, \vec{B}^\perp denotes the vector perpendicular to \vec{B} . The left (right) cylinder has L_1 ($L_1 - 1$) surface unit-cells.

spectrum are present only in crystal with globally centrosymmetric unit cells.

Similarly, the fact that the charge polarization of a crystal accounts for both its ionic and electronic contributions makes it impossible to uniquely probe the crystalline electronic topology.

The aim of this Letter is to show that dislocation charge unequivocally reveal the topology of two-dimensional crystals protected by inversion and rotation symmetries. Using a relation between the dislocation charges and the (partial) Berry phases of the bulk crystals, we show indeed that in inversion- and rotation-symmetric insulators the dislocation charge always possesses a topological quantized contribution directly linked to bulk crystalline topological invariants. This correspondence holds both in the absence and in the presence of time-reversal symmetry, in which case we formulate new topological invariants.

Berry phase formulation of the dislocation charge – Dislocations are topological defects in crystals. They can be associated with a topological invariant, the Burgers vector \vec{B} , which measures the difference between a defect-free and a distorted crystal. It can be defined as follows: One first traces out a loop surrounding the defect clockwise, and subsequently transfers this loop to a defect-free lattice. Due to the dislocation, the loop will fail to close.

The vector that one needs to add to close the loop is the Burgers vector, see Fig. 1. The presence of this topological defect also produces a local distortion in the otherwise homogeneous charge distribution. For a conventional insulator, in fact, the charge per unit cell ρ_i in the vicinity of the dislocation core will deviate from its bulk value N_F , the number of occupied bands. Albeit the precise details of the charge distribution will depend on microscopic details, the dislocation charge Q , defined as the sum of the local charge deviations $\Delta\rho_i = \rho_i - N_F$, is a bulk quantity. More specifically, and as shown below, it can be related to the Berry connection $\mathcal{A}_j^{m,n}(\vec{q}) = \langle \Psi_m(\vec{q}) | i\partial_{q_j} | \Psi_n(\vec{q}) \rangle$, where $|\Psi_m(\vec{q})\rangle$ denotes a Bloch wave with band index m and momentum \vec{q} .

To derive such a relation, let us imagine that the dislocation is obtained by gluing two cylinders with different surface unit cells, as shown in Fig. 1. Since the total charge must be integer, we find that the dislocation charge (modulo 1) can be related to the edge charges of these cylinders via $Q = -Q_L - Q_R$, with $Q_{L(R)}$ the total left (right) edge charge. Both cylinders are periodic in the \vec{a}_1 direction, and thus can be viewed as a collection of 1D systems parametrized by $q_1 = j2\pi/L_1$ and $q_1 = j2\pi/(L_1 - 1)$, respectively. This, in turns, allows us to express Q in terms of the corresponding Berry phases $\gamma_2(q_1) = \int_0^{2\pi} dq_2 \text{Tr}[\mathcal{A}_2(\vec{q})]$, see Refs. [27, 28]. In the $L_1 \rightarrow \infty$ limit, we then find [see the Supplemental Material] that the dislocation charge is given by

$$Q = \frac{1}{2\pi} \int_0^{2\pi} dq_1 \gamma_2(q_1) =: \frac{\gamma_2}{2\pi} \text{ modulo } 1. \quad (1)$$

In obtaining Eq. (1), we have used that $\gamma_2(q_1)$ depends continuously on q_1 . Moreover we stress that while in trivial insulators one may freely change the domain of integration to $[\phi, \phi + 2\pi]$, in topological insulators with non-zero Chern number (Ch), such a change of integration domain changes the dislocation charge as $\gamma_2 \rightarrow \gamma_2 + Ch\phi$. This, however, should not surprise since a change in the domain of integration corresponds to the situation where an external magnetic flux ϕ is threading the dislocation core, and thus an additional contribution $\phi/(2\pi)$ to the dislocation charge is totally expected. Finally, repeating the analysis above for a dislocation with Burgers vector $\vec{B} = \vec{a}_2$ yields the general expression for the dislocation charge $Q = \vec{B}^\perp \cdot \vec{\gamma}/(2\pi)$ modulo 1, with $\vec{\gamma} = [\gamma_1 \vec{a}_1 + \gamma_2 \vec{a}_2] / \|\vec{a}_1 \times \vec{a}_2\|$ representing a Berry phase vector, and \vec{B}^\perp the vector perpendicular to \vec{B} .

Let us next consider a time-reversal symmetric system with $\hat{T}^2 = -1$. Then Kramers theorem guarantees that every state is doubly degenerate. In particular, this applies to states bound to the dislocation core. Hence, in the presence of time-reversal symmetry the dislocation charge has to be well-defined modulo 2. To account for this, we first note that the edge charges associated with the momenta q_1 and $-q_1$ are identical.

Moreover, for $q_1 = 0, \pi$, the corresponding 1D Hamiltonian is time-reversal symmetric. Hence, along these 1D cuts we can group the eigenstates in Kramers pairs $|\Psi_m^I(\vec{q})\rangle = e^{i\phi_m(\vec{q})} \tilde{T} |\Psi_m^{II}(-\vec{q})\rangle$. The superscript $\alpha = I, II$ labels the two time-reversed "channels" and \tilde{T} denotes the first-quantized time-reversal operator. Using the results from Ref. [27] it follows that the corresponding edge charge is then given by $\gamma^I(q_1)/\pi$. Here, $\gamma^I(q_1)$ is the partial Berry phase, which is simply the Berry phase calculated for a single time-reversed channel. Combining these results, we find

$$Q = \frac{1}{2\pi^2} \int_0^\pi dq_1 \gamma_2(q_1) + \frac{1}{\pi} \gamma_2^I(\pi) - \frac{1}{2\pi} \gamma_2(\pi) \\ =: \frac{\gamma_2^I}{\pi} \text{ modulo } 2, \quad (2)$$

and for a generic dislocation we can then write $Q = \vec{B}^\perp \cdot \vec{\gamma}^I/\pi$ modulo 2, with $\vec{\gamma}^I$ the partial Berry phase vector.

Inversion- and n-fold rotation-symmetric insulators –

Having established the relation between the dislocation charge and the (partial) Berry phases, we now discuss the topological invariants associated to 2D crystalline insulators in the presence of inversion and/or rotational symmetries without time-reversal symmetry, see also Refs. [24, 25, 29–31]. First we note that the topological invariants associated to these spatial symmetries cannot always be uniquely defined. This follows from the fact that when considering inversion and rotational symmetries, one can define multiple inversion centers or rotation axes per unit-cell. For example, inversion-symmetric crystals host four inversion centers per unit-cell and threefold rotation symmetric insulators exhibit three rotation axes per unit-cell [c.f. Figs. 2(a) and (b)]. Let us analyze the consequences of this for inversion-symmetry, and consider the inversion operator corresponding to the inversion center A shown in Fig. 2(a). An electron in the \vec{i} th unit-cell and belonging to partition \mathcal{A} will be mapped to the $-\vec{i}$ th unit-cell. However, electrons belonging to partitions \mathcal{B} , \mathcal{C} , or \mathcal{D} are sent to unit cells $-\vec{i} - (1, 0)$, $-\vec{i} - (1, 1)$, or $-\vec{i} - (0, 1)$, respectively. As a consequence, we find that the Fourier transformed inversion operator is momentum dependent: $\tilde{I}_A(\vec{q}) = \text{diag}(\tilde{I}_A, e^{-iq_1} \tilde{I}_B, e^{-i(q_1+q_2)} \tilde{I}_C, e^{-iq_2} \tilde{I}_D)$. Performing a similar analysis for the other inversion centers yields that all inversion operators are equal up to \vec{q} -dependent phase factors, *i.e.* $\tilde{I}_A(\vec{q}) = e^{-iq_1} \tilde{I}_B(\vec{q}) = e^{-i(q_1+q_2)} \tilde{I}_C(\vec{q}) = e^{-iq_2} \tilde{I}_D(\vec{q})$. Henceforth, topological invariants associated with inversion symmetry are all linked to each other. But a topological index that is coined to be non-trivial with respect to one inversion center, may be trivial with respect to another inversion center, and vice versa.

The topological index can be identified by introducing the sewing matrix $\mathcal{S}_{IA}^{m,n}(\vec{q}) := \langle \Psi_m(-\vec{q}) | \tilde{I}_A(\vec{q}) | \Psi_n(\vec{q}) \rangle$, with $m, n = 1, \dots, N_F$, and where we chose the inver-

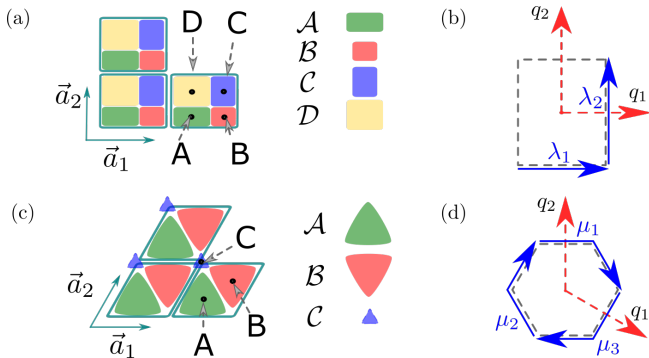


FIG. 2: Real-space and momentum space structure of inversion and rotationally invariant crystals. (a) Generic inversion-symmetric crystal. (b) Corresponding Brillouin zone with the two contours λ_1 and λ_2 along high-symmetry lines. (c) Generic threefold rotationally symmetric crystal. (d) Corresponding Brillouin zone, with the contours μ_1 , μ_2 and μ_3 along high-symmetry lines.

sion center A for convenience. This matrix tracks how the occupied states at \vec{q} and $-\vec{q} = I\vec{q}$ are related by inversion symmetry. As long as the inversion operator commutes with the Hamiltonian, $\mathcal{S}_{\vec{I}_A}$ is a unitary matrix, and one can consider the winding number of the corresponding determinant along an arbitrary closed contour C : $W_C(\mathcal{S}_{\vec{I}_A}) := \frac{i}{2\pi} \int_C d\vec{q} \cdot \nabla \log \det \mathcal{S}_{\vec{I}_A}(\vec{q}) \in \mathbb{Z}$. For a generic contour this integer is gauge dependent since under an arbitrary gauge transformation $|\Psi_m(\vec{q})\rangle \rightarrow \mathcal{U}_{m,n}(\vec{q})|\Psi_n(\vec{q})\rangle$, we have that $W_C(\mathcal{S}_{\vec{I}_A}) \rightarrow W_C(\mathcal{S}_{\vec{I}_A}) + W_C(\mathcal{U}) + W_{IC}(\mathcal{U}^*)$. For contours that change orientation under inversion, i.e. $IC = -C$, the winding number can only change by a multiple of 2, and as such it defines a \mathbb{Z}_2 invariant [32]. In particular, we may consider the two contours λ_1 and λ_2 , depicted in Fig. 2(b). The integrand for the winding number is even along these contours, and therefore we can express both \mathbb{Z}_2 -invariants in terms of the determinants at the inversion-invariant momenta

$$\xi_{i=1,2,I_A} := e^{-i\pi W_{\lambda_i}(\mathcal{S}_{\vec{I}_A})} = \frac{\det \mathcal{S}_{\vec{I}_A}(M)}{\det \mathcal{S}_{\vec{I}_A}(X_i)}.$$

Inversion symmetry therefore endows two-dimensional crystalline insulators with a $\mathbb{Z}_2 \times \mathbb{Z}_2$ topology [25]. Clearly, the same analysis can be performed for C_2 -invariant insulators, in which case the corresponding invariants can be labeled as $\xi_{1,C_2,A}$ and $\xi_{2,C_2,A}$.

The unique signature of these topological invariants does not reside in the presence of anomalous edge states but can be rather identified using their one-to-one correspondence to the Berry vector, and consequently to a generic dislocation charge. Using that the sum of the Berry connection at \vec{q} and $-\vec{q}$ can be expressed in terms of the sewing matrix $\mathcal{S}_{\vec{I}_A}(\vec{q})$ and the charges in the partitions \mathcal{B} , \mathcal{C} , and \mathcal{D} , we find that [see the Supplemental

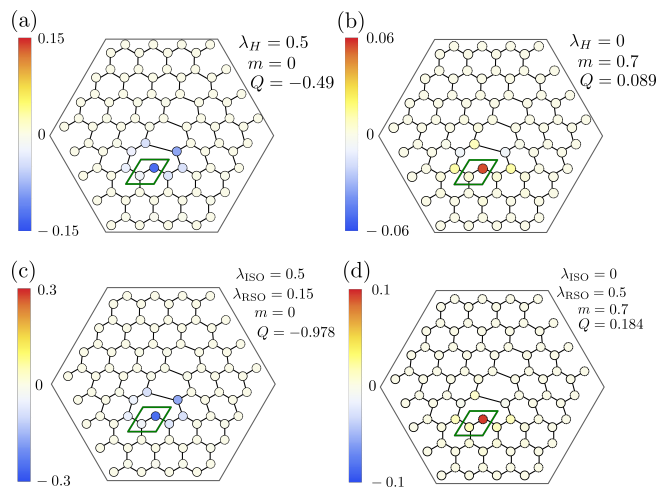


FIG. 3: Edge dislocation with Burgers vector $\vec{B} = \vec{a}_1$. The color quantifies the charge local charge deviation. The inset depicts the parameters that have been used, and Q corresponds to the sum of the charge deviations within the hexagon. The upper-panels corresponds to a spinless honeycomb lattice, whereas the lower panels include spin-orbit coupling terms. In all cases we use $t = 1$.

Material]

$$\gamma_{1/2} = i \log(\xi_{1/2,I_A}) - \pi [\rho_{\mathcal{B}/\mathcal{D}} + \rho_{\mathcal{C}}] \quad (3)$$

Hence, for a generic dislocation, we find that the charge consists of two parts, one quantized to 0 or 1/2 and a second part which typically is unquantized. Observe that the charge in the \mathcal{B} , \mathcal{C} , and \mathcal{D} partitions can be independently identified in the bulk. This proves that the dislocation charge probes the crystalline topology.

In a similar fashion, one can study the electronic topology of C_3 -symmetric crystals. Then each unit-cell will host 3 rotation axes, which we label as A, B, and C, see Fig. 2. Again, we limit ourselves to rotation axis A. One can show that the winding number of the sewing matrix $\mathcal{S}_{\vec{C}_{3,A}}$ along the contour $\mu_1 - \mu_3$ defines a \mathbb{Z}_3 invariant:

$$\xi_{\mathcal{C}_{3,A}} = e^{-i\frac{2\pi}{3} W_{\mu_1 - \mu_3}(\mathcal{S}_{\vec{C}_{3,A}})} = \frac{\det \mathcal{S}_{\vec{C}_{3,A}}(K^+)}{\det \mathcal{S}_{\vec{C}_{3,A}}(K^-)}$$

with $K^\pm = \pm(2\pi/3, 4\pi/3)$. Next, we use that the Berry connections at \vec{q} , $R\vec{q}$, and $R^2\vec{q}$ are related to each other by the sewing matrix, with R the rotation matrix corresponding to an anti-clockwise rotation of $2\pi/3$ [33]. This allows us to write

$$\begin{aligned} \gamma_1 &= i \log(\xi_{\mathcal{C}_{3,A}}) - 2\pi[\rho_{\mathcal{B}} - \rho_{\mathcal{C}}]/3, \text{ and} \\ \gamma_2 &= i \log(\xi_{\mathcal{C}_{3,A}}) - 2\pi[\rho_{\mathcal{B}} + 2\rho_{\mathcal{C}}]/3. \end{aligned} \quad (4)$$

In this case, we find that the topological contribution to the dislocation charge is quantized to multiples of 1/3.

Honeycomb lattice model – To illustrate the results above, we consider an honeycomb lattice with a dislocation characterized by the Burgers vector $\vec{B} = \vec{a}_1$. In the lattice model, the electrons can hop between neighboring sites with a hopping parameter t , experience a staggered sub-lattice potential $\pm m$, and we include a time-reversal symmetry breaking term corresponding to chiral orbital currents [4]. In the tight-binding formulation the latter yields imaginary next-nearest neighbor hopping processes. In momentum space, the bulk Hamiltonian reads:

$$\tilde{H}(\vec{q}) = \begin{pmatrix} m + f(\vec{q}) & -t(1 + e^{-iq_1} + e^{-iq_2}) \\ -t(1 + e^{iq_1} + e^{iq_2}) & -m - f(\vec{q}) \end{pmatrix}$$

with $f(\vec{q}) = 2\lambda_H[\sin(q_1) - \sin(q_2) + \sin(q_2 - q_1)]$. We first set $m = 0$, in which case the system is inversion-symmetric, with the inversion operator given by the first Pauli matrix τ_1 . Its matrix representation is momentum independent since the unit cell is globally inversion-symmetric. At half-filling we find $\xi_{1,I_A} = \xi_{2,I_A} = -1$ and hence for the dislocation depicted in Fig. 3(a), Eqs. (1) and (3) predict a dislocation charge $Q = 1/2$. We have numerically verified this result by computing the local charge around the dislocation as indicated in Fig. 3. We have also analyzed the effect of the inversion-symmetry breaking term reducing the crystal symmetry to C_3 . The rotation operator has the matrix representation $\tilde{C}_{3,A}(\vec{q}) = \text{diag}(1, e^{-iq_2})$, and acquires a momentum dependence since the unit-cell is not rotation-symmetric. At half-filling the \mathbb{Z}_3 invariant is given by

$$\xi_{C_{3,A}} = \begin{cases} 1 & \text{if } m < -3\sqrt{3}|\lambda_H| \\ e^{i2\pi/3} & \text{if } -3\sqrt{3}|\lambda_H| < m < 3\sqrt{3}|\lambda_H| \\ e^{-i2\pi/3} & \text{if } m > 3\sqrt{3}|\lambda_H| \end{cases}$$

Let us analyze the case $\lambda_H = 0$ and $m = 0.7t$. We have numerically calculated the charge in the \mathcal{B} partition, which is given by $\rho_B = 0.73$. Hence, using Eqs. (1) and (4) we predict $Q = 1/3 - 0.73/3 = 0.09$, which is in perfect agreement with the result shown in Fig. 3(b).

Time-reversal symmetry – In time-reversal symmetric systems, Kramer's theorem guarantees that inversion- and C_2 -symmetric crystals cannot be characterized topologically by the $\mathbb{Z}_2 \times \mathbb{Z}_2$ -invariants introduced above. This follows from the fact that at the time-reversal invariant momenta the determinant of the sewing matrices is always 1. However, this does not preclude the existence of a different topology. In order to define such new topological invariants, we consider the winding number of the determinants over half the contour $\lambda_{1(2)}$, i.e. from $X_{2(1)}$ to M . In general, this winding number is gauge dependent. However, if we impose a time-reversal symmetric gauge along these contours then both yield a \mathbb{Z}_2 -invariant [27, 29]. We denote these winding numbers with $W_{\lambda_i}^{1/2}(\mathcal{S}_{\tilde{I}(\tilde{C}_2)_A})$. In inversion-symmetric insulators, we can simply express this invariant in terms of the eigenvalues of the inversion-operator for half of the Kramers

partners:

$$\chi_{i,\tilde{I}_A} := e^{-i\pi W_{\lambda_i}^{1/2}(\mathcal{S}_{\tilde{I}_A})} = \det \mathcal{S}_{\tilde{I}_A}^I(M) / \mathcal{S}_{\tilde{I}_A}^I(X_i)$$

Here, \mathcal{S}^I denotes the restriction of the sewing matrix to a single time-reversed "channel". For C_2 -symmetric insulators, instead, such a simple expression does not exist. This difference stems from the fact that $(\hat{I}\hat{T})^2 = -1$ and $(\tilde{C}_2\tilde{T})^2 = 1$. Similarly to the discussion above, we find the following relation between the partial Berry phase and these topological invariants:

$$\gamma_{1/2}^I = i \log(\chi_{1/2,\tilde{X}_A}) - \pi[\rho_{B/D} + \rho_C]/2, \quad (5)$$

with $X = I$ or C_2 . The \mathbb{Z}_3 -topology does not suffer the same fate in the presence time-reversal symmetry, for the very simple fact that $1 + 1 \neq 0$ modulo 3. Since K^+ and K^- are related by time-reversal symmetry, it follows that we can simplify the expression for ξ_{C_3} , by writing

$$\xi_{C_{3,A}} = \det \mathcal{S}_{\tilde{C}_{3,A}}(K^+) =: \chi_{C_{3,A}}^2.$$

On the right-hand side we have introduced the invariant $\chi_{C_{3,A}}$. Although this invariant does not encode any new information, it is $\chi_{C_{3,A}}$ that is directly related to the partial Berry phase. Namely, we can impose a time-reversal symmetric gauge along the contours μ_i and compute the winding numbers $W_{\mu_1}^{1/2}$ and $W_{\mu_3}^{1/2}$, from X_2 to M , and from X_1 to M , respectively. Then it follows [see Supplemental Material], that the winding number $W_{\mu_1 - \mu_3}^{1/2}(\mathcal{S}_{\tilde{C}_{3,A}})$ is directly related to $\chi_{C_{3,A}}$ as

$$W_{\mu_1 - \mu_3}^{1/2}(\mathcal{S}_{\tilde{C}_{3,A}}) = \frac{3}{2\pi} i \log(\chi_{C_{3,A}}).$$

This, in turns, allows us to express the partial Berry vector solely in terms of $\chi_{C_{3,A}}$, ρ_B , and ρ_C :

$$\begin{aligned} \gamma_1^I &= i \log(\chi_{C_{3,A}}) - \pi[\rho_B - \rho_C]/3 \text{ and} \\ \gamma_2^I &= i \log(\chi_{C_{3,A}}) - \pi[\rho_B + 2\rho_C]/3. \end{aligned} \quad (6)$$

Spinful honeycomb lattice model – To demonstrate these results we consider a time-reversal symmetric honeycomb lattice model for spin-one-half fermions, where we include both intrinsic and Rashba spin-orbit coupling [6]. The former corresponds to spin-dependent chiral orbital currents, whereas the latter leads to nearest-neighbor hoppings that flip the spin [see the Supplemental Material]. It is easily verified that both terms respect the C_3 and C_2 -symmetry. For the latter, the corresponding symmetry operators reads:

$$\tilde{C}_{2,A}(\vec{q}) = \tau_1 \otimes i\sigma_3 \text{ and } \tilde{C}_{3,A}(\vec{q}) = \text{diag}(1, e^{-iq_2}) \otimes e^{i\frac{\pi\sigma_3}{3}}$$

For the example depicted in Fig. 3(c) we find $\chi_{1,C_{2,A}} = \chi_{2,C_{2,A}} = -1$, which yields $Q = 1$ modulo 2. This result is numerically confirmed. In Fig. 3(d) we have depicted

a spinful C_3 -symmetric crystal. Using these parameters we find $\chi_{C_{3,A}} = e^{-i2\pi/3}$. Moreover, we find that $\rho_B = 1.44$. Therefore, we predict $Q = 2/3 - \rho_B/3 = 0.187$. Again, this is in perfect agreement with the result shown in Fig. 3(d).

Conclusions – To conclude, we have shown that the fractional part of the dislocation charge is a bulk property that can be linked to the Berry phase. In time-reversal symmetric systems, one can link the dislocation charge to the partial Berry phase, and microscopic details can only change the charge by multiples of 2. We have also shown that in inversion- and rotation symmetric insulators, one can express the (partial) Berry phases in terms of topological crystalline invariants. Topological defects generally allow to identify non-trivial states of matter both in superconductors [30, 31] and in insulators [34–38]. Our results establish on firm grounds that dislocation charges uniquely probe topological crystalline insulators protected only by spatial symmetries.

Acknowledgements – C.O. acknowledges support from a VIDI grant (Project 680-47-543) financed by the Netherlands Organization for Scientific Research (NWO). This work is part of the research programme of the Foundation for Fundamental Research on Matter (FOM), which is part of the Netherlands Organization for Scientific Research (NWO).

[1] M. Z. Hasan and C. L. Kane, *Rev. Mod. Phys.* **82**, 3045 (2010).
 [2] X.-L. Qi and S.-C. Zhang, *Rev. Mod. Phys.* **83**, 1057 (2011).
 [3] D. J. Thouless, M. Kohmoto, M. P. Nightingale, and M. den Nijs, *Phys. Rev. Lett.* **49**, 405 (1982).
 [4] F. D. M. Haldane, *Phys. Rev. Lett.* **61**, 2015 (1988).
 [5] K. von Klitzing, G. Dorda, and M. Pepper, *Phys. Rev. Lett.* **45**, 494 (1980).
 [6] C. L. Kane and E. J. Mele, *Phys. Rev. Lett.* **95**, 226801 (2005).
 [7] C. L. Kane and E. J. Mele, *Phys. Rev. Lett.* **95**, 146802 (2005).
 [8] B.A. Bernevig, T.L. Hughes, and S.-C. Zhang, *Science* **314**, 1757 (2006).
 [9] M. König, S. Wiedmann, C. Brüne, A. Roth, H. Buhmann, L.W. Molenkamp, X.-L. Qi, and S.-C. Zhang, *Science* **318**, 766 (2007).
 [10] L. Fu, C.L. Kane, and E.J. Mele, *Phys. Rev. Lett.* **98**, 106803 (2007).
 [11] J.E. Moore and L. Balents, *Phys. Rev. B* **75**, 121306(R) (2007).
 [12] L. Fu and C. L. Kane, *Phys. Rev. B* **76**, 045302 (2007).
 [13] H.J. Zhang, C.-X. Liu, X.-L. Qi, Z. Fang, and S.-C. Zhang, *Nat. Phys.* **5**, 438 (2009).

[14] C.-X. Liu, X.-L. Qi, H.J. Zhang, X. Dai, Z. Fang, and S.-C. Zhang, *Phys. Rev. B* **82**, 045122 (2010).
 [15] B. Rasche, A. Isaeva, M. Ruck, S. Borisenko, V. Zabolotnyy, B. Büchner, K. Koepf, C. Ortix, M. Richter, and J. van den Brink, *Nat. Mater.* **12**, 422 (2013).
 [16] L. Fu, *Phys. Rev. Lett.* **106**, 106802 (2011).
 [17] T.H. Hsieh, H. Lin, J. Liu, W. Duan, A. Bansil, and L. Fu, *Nat. Commun.* **3**, 982 (2012).
 [18] Y. Ando and L. Fu, *Ann. Rev. Condens. Matter Phys.* **6**, 361 (2015).
 [19] D. Hsieh, D. Qian, L. Wray, Y. Xia, Y.S. Hor, R.J. Cava, and M.Z. Hasan, *Nature* **452**, 970 (2008).
 [20] Y. Xia, D. Qian, D. Hsieh, L. Wray, A. Pal, H. Lin, A. Bansil, D. Grauer, Y. S. Hor, R.J. Cava, and M.Z. Hasan, *Nat. Phys.* **5**, 398 (2009).
 [21] Y.L. Chen, J.G. Analytis, J.-H. Chu, Z. K. Liu, S.-K. Mo, X. L. Qi, H. J. Zhang, D. H. Lu, X. Dai, Z. Fang, S. C. Zhang, I.R. Fisher, Z. Hussain, and Z.-X. Shen, *Science* **325**, 178 (2009).
 [22] D. Hsieh, Y. Xia, L. Wray, D. Qian, A. Pal, J. H. Dil, J. Osterwalder, F. Meier, G. Bihlmayer, C. L. Kane, Y. S. Hor, R.J. Cava, M.Z. Hasan, *Science* **323**, 919 (2009).
 [23] Y. Tanaka, Z. Ren, T. Sato, K. Nakayama, S. Souma, T. Takahashi, K. Segawa, Y. Ando, *Nat. Phys.* **8**, 800 (2012).
 [24] T.L. Hughes, E. Prodan, B.A. Bernevig, *Phys. Rev. B* **83**, 245132 (2011).
 [25] C. Fang, M. J. Gilbert, and B.A. Bernevig, *Phys. Rev. B* **86** 115112 (2012).
 [26] P. Jadaun, D. Xiao, Q. Niu, and S.K. Banerjee, *Phys. Rev. B* **88**, 085110 (2013).
 [27] G. van Miert and C. Ortix, *Phys. Rev. B* **96**, 235130 (2017).
 [28] J.W. Rhim, J. Behrends, J.H. Bardarson, *Phys. Rev. B* **95**, 035421 (2017).
 [29] A. Lau, J. van den Brink, and C. Ortix, *Phys. Rev. B* **94**, 165164 (2016).
 [30] J.C.Y. Teo and T.L. Hughes, *Phys. Rev. Lett.* **111**, 047006 (2013).
 [31] W.A. Benalcazar, J.C.Y. Teo, and T.L. Hughes, *Phys. Rev. B* **89**, 224503 (2014).
 [32] Here, we have used that $W_{-C}(\mathcal{U}^*) = W_C(\mathcal{U})$.
 [33] The rotation matrix reads

$$R = \begin{pmatrix} 0 & -1 \\ 1 & -1 \end{pmatrix}.$$

[34] Y. Ran, Y. Zhang, and A. Vishwanath, *Nat. Phys.* **5**, 298 (2009).
 [35] W.A. Benalcazar, B.A. Bernevig, and T. Hughes, *Science* **357**, 61 (2017).
 [36] W.A. Benalcazar, B.A. Bernevig, and T.L. Hughes, *Phys. Rev. B* **96**, 245115 (2017).
 [37] F. de Juan, A. Rüegg, and D.-H. Lee, *Phys. Rev. B* **89**, 161117(R) (2014).
 [38] V. Juričić, A. Mesáros, R.-J. Slager, and J. Zaanen, *Phys. Rev. Lett.* **108**, 106403 (2012).

SUPPLEMENTAL MATERIAL

NOTATION

In this section we introduce our notation and conventions. We consider a 2D Bravais lattice with primitive vectors \vec{a}_1 and \vec{a}_2 , see Fig. 1. Accordingly, we label the unit cells with an integer vector $\vec{j} = (j_1, j_2)$. Then, we can write a generic tight-binding Hamiltonian as

$$\hat{H} = \sum_{\vec{i}, \vec{j}} \sum_{\alpha, \beta} t_j^{\alpha, \beta} f_{i, \alpha}^\dagger f_{i+\vec{j}, \beta},$$

where $f_{i, \alpha}^\dagger$ is the creation operator corresponding to an electron in unit-cell \vec{i} , and the index α , which runs from 1 to N refers to the electronic internal degrees of freedom and may therefore correspond to a spin, a sublattice or an orbital index. For example, in the example of the honeycomb lattice it refers to the sublattice index. The choice of the unit cell is fixed by the dislocation under consideration, see for example Fig. 3 where the green rectangle denotes a preferred unit cell. To exploit the translation symmetry, we introduce the Fourier transformed creation and annihilation operators

$$f_{\vec{q}, \alpha}^\dagger := \sum_{l_1=1}^{L_1} \sum_{l_2=1}^{L_2} e^{i\vec{q} \cdot \vec{l}} f_{l, \alpha}^\dagger / \sqrt{L_1 L_2}.$$

Note that $\vec{q} \cdot \vec{l} = (q_1 \vec{b}_1 + q_2 \vec{b}_2) \cdot (l_1 \vec{a}_1 + l_2 \vec{a}_2) / (2\pi)$, where \vec{b}_1 and \vec{b}_2 denote the reciprocal lattice vectors. Using these operators we can rewrite the Hamiltonian as

$$\hat{H} = \sum_{\vec{q} \in BZ} \hat{H}(\vec{q}) = \sum_{\alpha, \beta} \sum_{\vec{q} \in BZ} f_{\vec{q}, \alpha}^\dagger \tilde{H}^{\alpha, \beta}(\vec{q}) f_{\vec{q}, \beta},$$

where $\tilde{H}^{\alpha, \beta}(\vec{q}) = \sum_{\vec{j}} t_j^{\alpha, \beta} e^{i\vec{q} \cdot \vec{j}}$. We refer to $\hat{H}(\vec{q})$ as the second-quantized Hamiltonian, while $\tilde{H}(\vec{q})$ is its first quantized counterpart. We mention that we will use the same notation for other operators that we will introduce throughout this paper. We further denote the eigenstates of the first quantized Hamiltonian with $|\Psi_n(\vec{q})\rangle = [\Psi_{n,1}(\vec{q}), \dots, \Psi_{n,N}(\vec{q})]^T$, where $n = 1, \dots, N$ is the band index. The real-space wave function with crystal momentum q and band index n within a given unit cell is proportional to $|\Psi_n(q)\rangle$. Finally, we need to define the Berry connection

$$\mathcal{A}_j^{m,n}(\vec{q}) = \langle \Psi_m(\vec{q}) | i \partial_{q_j} | \Psi_n(\vec{q}) \rangle,$$

with $m, n = 1, \dots, N_F$, and the Abelian part of the Berry curvature, which is given by

$$\mathcal{F}_{i,j} = \partial_{q_i} \text{Tr} \mathcal{A}_j(\vec{q}) - \partial_{q_j} \text{Tr} \mathcal{A}_i(\vec{q})$$

The Berry phase γ_λ corresponding to a generic contour λ is defined as

$$\gamma_\lambda = \int_\lambda d\vec{q} \cdot \text{Tr} [\vec{\mathcal{A}}(\vec{q})].$$

If the contour is time-reversal symmetric, and $\hat{T}^2 = -1$, then one can consider the partial Berry phase γ_λ^I , which is defined as

$$\gamma_\lambda^I = \int_{\lambda^{1/2}} d\vec{q} \cdot \text{Tr} [\vec{\mathcal{A}}(\vec{q})],$$

here $\lambda^{1/2}$ denotes half of the contour λ , and the union with the time-reversal copy, makes up the full contour λ . Moreover, it is required that one evaluates this contour integral using a time-reversal symmetric gauge: $|\Psi_n^I(\vec{q})\rangle = \tilde{T} |\Psi_n^{II}(-\vec{q})\rangle$, see also Refs. 12, 27. In principle one may drop this constraint, by writing

$$\gamma_\lambda^I = \int_{\lambda^{1/2}} d\vec{q} \cdot \text{Tr} [\vec{\mathcal{A}}(\vec{q})] + i \log \left(\frac{\text{Pf} \mathcal{S}_{\tilde{T}}(\lambda_f^{1/2})}{\text{Pf} \mathcal{S}_{\tilde{T}}(\lambda_i^{1/2})} \right),$$

where $\lambda_{i(f)}^{1/2}$ denotes the time-reversal invariant starting (end) point of the contour $\lambda^{1/2}$.

DETAILED DERIVATIONS OF THE MAIN RESULTS

Below we provide detailed derivations of the main results.

Derivation of Eq. (1)

As discussed in the main text, we can express the dislocation charge in terms of the left and right edge charge of the two cylinders shown in Fig. 1 $Q = -Q_L - Q_R$. Hence, we simply need to calculate both separately. We note that both edges shown in Fig. 1 are translation symmetric in the direction \vec{a}_1 . Hence, we may write

$$Q_L = \sum_{j=0}^{L_1-1} Q_L \left(\frac{j2\pi}{L_1} \right) \quad \text{and} \quad Q_R = \sum_{j=0}^{L_1-2} Q_R \left(\frac{j2\pi}{L_1-1} \right),$$

where $Q_{L(R)}(q_1)$ denotes the left (right) edge charge for a 1D insulator governed by the 1D Hamiltonian $\hat{H}_{q_1}(q_2) := \hat{H}(q_1, q_2)$. In Refs. 27, 28, it has been shown that for a 1D crystalline insulator the right (left) edge charge is given by $+(-)\gamma/(2\pi)$, with

$$\gamma = \sum_{n \leq N_F} \int_0^{2\pi} dq \langle \Psi_n(q) | i\partial_q | \Psi_n(q) \rangle.$$

Therefore, we find

$$Q_L = -\frac{1}{2\pi} \sum_{j=0}^{L_1-1} \gamma_2 \left(\frac{j2\pi}{L_1} \right) \quad \text{and} \quad Q_R = \frac{1}{2\pi} \sum_{j=0}^{L_1-2} \gamma_2 \left(\frac{j2\pi}{L_1-1} \right)$$

with

$$\gamma_2(q_1) = \int_0^{2\pi} dq_2 \langle \Psi_n(q_1, q_2) | i\partial_{q_2} | \Psi_n(q_1, q_2) \rangle = \int_0^{2\pi} dq_2 \text{Tr} [\mathcal{A}_2(\vec{q})].$$

As a result, we obtain the following expression for the dislocation charge:

$$Q = \frac{1}{2\pi} \sum_{j=0}^{L_1-1} \gamma_2 \left(\frac{j2\pi}{L_1} \right) - \frac{1}{2\pi} \sum_{j=0}^{L_1-2} \gamma_2 \left(\frac{j2\pi}{L_1-1} \right) = \frac{1}{2\pi} \sum_{j=0}^{L_1-1} \left[\gamma_2 \left(\frac{j2\pi}{L_1} \right) - \gamma_2 \left(\frac{j2\pi}{L_1-1} \right) \right] + \frac{1}{2\pi} \gamma_2(2\pi)$$

To make further progress, we use that $\gamma_2(q + \delta q) - \gamma_2(q) \approx \gamma_2'(q)\delta q$. We then find:

$$Q \approx \frac{1}{2\pi} \sum_{j=0}^{L_1-1} \gamma_2' \left(\frac{j2\pi}{L_1} \right) \frac{j2\pi}{L_1} \frac{-1}{L_1-1} + \frac{1}{2\pi} \gamma_2(2\pi) \approx -\frac{1}{(2\pi)^2} \int_0^{2\pi} dq_1 \gamma_2'(q_1) q_1 + \frac{1}{2\pi} \gamma_2(2\pi) = \frac{1}{(2\pi)^2} \int_0^{2\pi} dq_1 \gamma_2(q_1)$$

In the final line, we have used partial integration. In the limit, $L_1 \rightarrow \infty$ the approximations become exact.

Derivation of Eq. (2)

In the presence of time-reversal symmetry, with $\hat{T}^2 = -1$, we can refine the argument presented above. Indeed, time-reversal symmetry ensures that $Q_{L(R)}(q_2) = Q_{L(R)}(-q_2)$. For the moment, let us assume that L_1 is even. Then, we find that the total left edge charge is given by

$$Q_L = 2 \sum_{j=1}^{L_1/2-1} Q_L \left(\frac{j2\pi}{L_1} \right) + Q_L(0) + Q_L(\pi) = -\frac{1}{\pi} \sum_{j=1}^{L_1/2-1} \gamma_2 \left(\frac{j2\pi}{L_1} \right) + Q_L(0) + Q_L(\pi)$$

For $q_1 = 0, \pi$, we find that the 1D Hamiltonian \hat{H}_{q_1} is time-reversal symmetric. Hence, the corresponding edge charge is well-defined modulo 2, see Ref. 27 and can be expressed in terms of the partial Berry phase

$$Q_L(0) = -Q_R(0) = -\frac{\gamma_2^I(0)}{\pi} = \frac{1}{\pi} \left[\int_0^\pi dq_2 \text{Tr} [\mathcal{A}_2(0, q_2)] + i \log \left(\frac{\text{Pf } \mathcal{S}_{\tilde{T}}(0, \pi)}{\text{Pf } \mathcal{S}_{\tilde{T}}(0, 0)} \right) \right] \text{ and}$$

$$Q_L(\pi) = -\frac{\gamma_2^I(\pi)}{\pi} = \frac{1}{\pi} \left[\int_0^\pi dq_2 \text{Tr} [\mathcal{A}_2(\pi, q_2)] + i \log \left(\frac{\text{Pf } \mathcal{S}_{\tilde{T}}(\pi, \pi)}{\text{Pf } \mathcal{S}_{\tilde{T}}(\pi, 0)} \right) \right]$$

Therefore, we find that the total left and right edge charges are given by

$$Q_L = -\frac{1}{\pi} \sum_{j=1}^{L_1/2-1} \gamma_2 \left(\frac{j2\pi}{L_1} \right) - \frac{\gamma_2^I(0)}{\pi} - \frac{\gamma_2^I(\pi)}{\pi} \text{ and } Q_R = \frac{1}{\pi} \sum_{j=1}^{L_1/2-1} \gamma_2 \left(\frac{j2\pi}{L_1-1} \right) + \frac{\gamma_2^I(0)}{\pi}.$$

From this it follows that the dislocation charge is given by

$$Q = \frac{1}{\pi} \sum_{j=1}^{L_1/2-1} \left[\gamma_2 \left(\frac{j2\pi}{L_1} \right) - \gamma_2 \left(\frac{j2\pi}{L_1-1} \right) \right] + \frac{\gamma_2^I(\pi)}{\pi},$$

Following the same steps as above, we end up with

$$Q = \frac{1}{2\pi^2} \int_0^\pi dq_1 \gamma_2(q_1) + \frac{\gamma_2^I(\pi)}{\pi} - \frac{\gamma_2(\pi)}{2\pi}$$

Useful identities

Here, we state important identities. Let I denote the inversion matrix, i.e. $I\vec{q} = -\vec{q}$. Then we find that for inversion-symmetric system the following identity holds:

$$|\Psi_m(I\vec{q})\rangle = \sum_{n \leq N_F} \mathcal{S}_{\tilde{I}_A}^\dagger(\vec{q})^{m,n} \tilde{I}_A(\vec{q}) |\Psi_n(\vec{q})\rangle, \text{ and } \langle \Psi_m(I\vec{q}) | = \sum_{n \leq N_F} \langle \Psi_n(\vec{q}) | \tilde{I}_A^\dagger(\vec{q}) \mathcal{S}_{\tilde{I}_A}(\vec{q})^{n,m}.$$

Let R denote the rotation matrix corresponding to an anti-clockwise rotation of $2\pi/3$:

$$R = \begin{pmatrix} 0 & -1 \\ 1 & -1 \end{pmatrix}.$$

Then, for C_3 -symmetric systems we find

$$|\Psi_m(R\vec{q})\rangle = \sum_{n \leq N_F} \mathcal{S}_{\tilde{C}_{3,A}}^\dagger(\vec{q})^{m,n} \tilde{C}_{3,A}(\vec{q}) |\Psi_n(\vec{q})\rangle, \text{ and } \langle \Psi_m(R\vec{q}) | = \sum_{n \leq N_F} \langle \Psi_n(\vec{q}) | \tilde{C}_{3,A}^\dagger(\vec{q}) \mathcal{S}_{\tilde{C}_{3,A}}(\vec{q})^{n,m}.$$

As states in the main text, we find that the inversion (two-fold rotation operator) generically is given by

$$\tilde{I}_A(\vec{q}) = \begin{pmatrix} \tilde{I}_A & 0 & 0 & 0 \\ 0 & \tilde{I}_B e^{-iq_1} & 0 & 0 \\ 0 & 0 & \tilde{I}_C e^{-i(q_1+q_2)} & 0 \\ 0 & 0 & 0 & \tilde{I}_D e^{-iq_2} \end{pmatrix}$$

and for C_3 -symmetric systems we obtain

$$\tilde{C}_{3,A}(\vec{q}) = \begin{pmatrix} \tilde{C}_{3,A} & 0 & 0 \\ 0 & \tilde{C}_{3,B} e^{-iq_2} & 0 \\ 0 & 0 & \tilde{C}_{3,C} e^{i(q_1-q_2)} \end{pmatrix}$$

As a result, we find

$$\tilde{I}_A(\vec{q})^\dagger i \partial_1 \tilde{I}_A(\vec{q}) = \begin{pmatrix} 0 & 0 & 0 & 0 \\ 0 & 1 & 0 & 0 \\ 0 & 0 & 1 & 0 \\ 0 & 0 & 0 & 0 \end{pmatrix} \text{ and } \tilde{I}_A(\vec{q})^\dagger i \partial_2 \tilde{I}_A(\vec{q}) = \begin{pmatrix} 0 & 0 & 0 & 0 \\ 0 & 0 & 0 & 0 \\ 0 & 0 & 1 & 0 \\ 0 & 0 & 0 & 1 \end{pmatrix}.$$

and

$$\tilde{C}_{3,A}(\vec{q})^\dagger i\partial_1 \tilde{C}_{3,A}(\vec{q}) = \begin{pmatrix} 0 & 0 & 0 \\ 0 & 0 & 0 \\ 0 & 0 & -1 \end{pmatrix} \text{ and } \tilde{C}_{3,A}(\vec{q})^\dagger i\partial_2 \tilde{C}_{3,A}(\vec{q}) = \begin{pmatrix} 0 & 0 & 0 \\ 0 & 1 & 0 \\ 0 & 0 & 1 \end{pmatrix}.$$

The identities allow us to relate the Berry connections at \vec{q} and $I\vec{q}$ through

$$\text{Tr}[\mathcal{A}(I\vec{q})] = I^T \left[\text{Tr}[\mathcal{A}(\vec{q})] + \vec{\rho}(\vec{q}) + i\nabla_{\vec{q}} \log \left(\det \mathcal{S}_{I_A}^\dagger(\vec{q}) \right) \right] \quad (7)$$

with $\vec{\rho}(\vec{q}) = (\rho_B(\vec{q}) + \rho_C(\vec{q}), \rho_C(\vec{q}) + \rho_D(\vec{q}))$. In addition we find that the Berry curvature satisfy

$$\mathcal{F}_{1,2}(I\vec{q}) = \mathcal{F}_{1,2}(\vec{q}) + \nabla \times \vec{\rho}(\vec{q}). \quad (8)$$

For C_3 -symmetric systems we find

$$\text{Tr}[\mathcal{A}(R\vec{q})] = (R^T)^2 \left[\text{Tr}[\mathcal{A}(\vec{q})] + \vec{\rho}(\vec{q}) + i\nabla_{\vec{q}} \log \left(\det \mathcal{S}_{\tilde{C}_{3,A}}^\dagger(\vec{q}) \right) \right], \quad (9)$$

with $\vec{\rho}(\vec{q}) = (-\rho_C(\vec{q}), \rho_B(\vec{q}) + \rho_C(\vec{q}))$. Which implies the following identity:

$$\mathcal{F}_{1,2}(R\vec{q}) = \mathcal{F}_{1,2}(\vec{q}) + \nabla \times \vec{\rho}(\vec{q}). \quad (10)$$

Derivation of Eq. (3)

To express γ_i in terms of the topological invariant ξ_{i,X_A} , with $X = C_2/I$, we first rewrite γ_1 :

$$\begin{aligned} \gamma_1 &= \frac{1}{2\pi} \int_0^{2\pi} dq_2 \gamma_1(q_2) = \gamma_1(0) + \frac{1}{2\pi} \int_0^{2\pi} dq_1 \int_0^{2\pi} dq_2 \mathcal{F}_{1,2}(\vec{q}) q_2 \\ &= \gamma_1(0) + \frac{1}{2\pi} \int_{-\pi}^{\pi} dq_1 \int_{-\pi}^{\pi} dq_2 \mathcal{F}_{1,2}(\vec{q}) q_2 + \int_{-\pi}^{\pi} dq_1 \int_{-\pi}^0 dq_2 \mathcal{F}_{1,2}(\vec{q}) = \gamma_1(\pi) + \frac{1}{2\pi} \int_{-\pi}^{\pi} dq_1 \int_{-\pi}^{\pi} dq_2 \mathcal{F}_{1,2}(\vec{q}) q_2 \end{aligned} \quad (11)$$

The expression on the RHS is completely gauge-invariant, i.e., it naturally implements the continuity constraint on $\gamma_1(q_2)$. Moreover, the domain is inversion-symmetric. Hence, we can take advantage of the fact that the Berry curvature at $-\vec{q}$ and \vec{q} are related through Eq. (8). Using this result we find

$$\gamma_1 = \gamma_1(\pi) - \pi [\rho_B + \rho_C] + \frac{1}{2} \int_{-\pi}^{\pi} dq_1 [\rho_C(q_1, \pi) + \rho_D(q_1, \pi)]$$

We can combine the first and last term using the results from Ref. 27. Then, we finally obtain

$$\gamma_1 = i \log(\xi_{1,X_A}) - \pi [\rho_B + \rho_C].$$

Derivation of Eq. (5)

Next, let us relate the invariant χ_{i,X_A} , with $X = C_2/I$, to the partial Berry phase γ_i^I . Again, we express the partial Berry phase in terms of the Berry curvature, i.e.

$$\gamma_1^I = \frac{1}{2\pi} \int_0^\pi dq_2 \gamma_1(q_2) + \gamma_1^I(\pi) - \gamma_1(\pi) = \frac{1}{2\pi} \int_0^{2\pi} dq_1 \int_0^\pi dq_2 \mathcal{F}_{1,2}(\vec{q}) q_2 + \gamma_1^I(\pi) = \frac{1}{4\pi} \int_{-\pi}^{\pi} dq_1 \int_{-\pi}^{\pi} dq_2 \mathcal{F}_{1,2}(\vec{q}) q_2 + \gamma_1^I(\pi),$$

where in the final equality we have used that $\mathcal{F}_{1,2}(\vec{q}) = -\mathcal{F}_{1,2}(-\vec{q})$ in the presence of time-reversal symmetry. Again, making use of Eq. (8) we obtain

$$\gamma_1^I = -\frac{\pi}{2} [\rho_B + \rho_C] + \frac{1}{4} \int_0^{2\pi} dq_1 [\rho_C(q_1, \pi) + \rho_D(q_1, \pi)] + \gamma_1^I(\pi) = i \log(\chi_{1,X_A}) - \frac{\pi}{2} [\rho_B + \rho_C].$$

The final equality is derived in Ref. 27 .

Relation $W_{\mu_1-\mu_3}(\mathcal{S}_{C_{3,A}})$ and $\det(\mathcal{S}_{\tilde{C}_{3,A}}(K^\pm))$

Here, we show that $W_{\mu_1-\mu_3}(\mathcal{S}_{C_{3,A}})$ can be expressed in terms of the determinant of the sewing matrix at the two high-symmetry points K^\pm . For this purpose we express the winding number in terms of the contours a , b , and c , shown in Fig. 1.

$$W_{\mu_1-\mu_3}(\mathcal{S}_{C_{3,A}}) = W_{2a+b-c}(\mathcal{S}_{C_{3,A}}).$$

Next, we use that

$$\nabla_{\vec{q}} \det \mathcal{S}_{\tilde{C}_{3,A}}(\vec{q}) \mathcal{S}_{\tilde{C}_{3,A}}(R\vec{q}) \mathcal{S}_{\tilde{C}_{3,A}}(R^2\vec{q}) = 0.$$

This allows us to write

$$W_{b-c}(\mathcal{S}_{C_{3,A}}) = W_a(\mathcal{S}_{C_{3,A}}),$$

where we have used that $b = -Ra$ and $c = R^2a$. Therefore, we can express the \mathbb{Z}_3 invariant in terms of the eigenvalues at the of the rotation operator at the high-symmetry points K^+ and K^- .

$$W_{\mu_1-\mu_3} = 3W_a = i \frac{3}{2\pi} \log \det(\mathcal{S}_{\tilde{C}_{3,A}}(K^+)/\det(\mathcal{S}_{\tilde{C}_{3,A}}(K^-))).$$

Relation $W_{\mu_1-\mu_3}^{1/2}(\mathcal{S}_{C_{3,A}})$ and $\det(\mathcal{S}_{\tilde{C}_{3,A}}(K^+))$

The argument presented above can also be used to relate $W_{\mu_1-\mu_3}^{1/2}(\mathcal{S}_{C_{3,A}})$ to the determinant of the sewing matrix at $\vec{q} = K^+$. For this purpose, we write:

$$W_{\mu_1-\mu_3}^{1/2}(\mathcal{S}_{C_{3,A}}) = W_{2a+b-c}^{1/2}(\mathcal{S}_{C_{3,A}}).$$

Then it follows that

$$W_{\mu_1-\mu_3}^{1/2}(\mathcal{S}_{C_{3,A}}) = 3W_a^{1/2}(\mathcal{S}_{C_{3,A}}) = i \frac{3}{2\pi} \log \det(\mathcal{S}_{\tilde{C}_{3,A}}(K^+)/\det(\mathcal{S}_{\tilde{C}_{3,A}}(0, \pi))) = i \frac{3}{2\pi} \log \det(\mathcal{S}_{\tilde{C}_{3,A}}(K^+)).$$

In the final equality we have made use of the fact that the determinant is identically equal to 1 at momenta that are time-reversal symmetric.

Derivation of Eq. (4)

In this section, we express γ_1 and γ_2 in terms of the invariant $\xi_{C_{3,A}}$. First, we will relate the integral of the Berry connection along the contour μ_1 to $\xi_{C_{3,A}}$. Making use of Eq. (9), we find

$$\begin{aligned} \gamma_{\mu_{i+1}} &= \int_{\mu_i} d(R\vec{q}) \cdot \text{Tr}[\mathcal{A}(R\vec{q})] = \int_{\mu_i} d\vec{q} \cdot \text{Tr}[\mathcal{A}(\vec{q})] + i \int_{\mu_i} d\vec{q} \cdot \nabla_{\vec{q}} \log(\det \mathcal{S}_{C_{3,A}}^\dagger(\vec{q})) + \int_{\mu_i} d\vec{q} \cdot \vec{\rho}(\vec{q}) \\ &= \gamma_{\mu_i} - 2\pi W_{\mu_i}(\mathcal{S}_{C_{3,A}}) + \int_{\mu_i} d\vec{q} \cdot \vec{\rho}(\vec{q}) \end{aligned}$$

As a result, we then obtain

$$\begin{aligned} \gamma_{\mu_1} &= \frac{1}{3} \left[\gamma_{\mu_1} + \gamma_{\mu_2} + 2\pi W_{\mu_1}(\mathcal{S}_{C_{3,A}}) - \int_{\mu_1} d\vec{q} \cdot \vec{\rho}(\vec{q}) + \gamma_{\mu_3} - 2\pi W_{\mu_3}(\mathcal{S}_{C_{3,A}}) + \int_{\mu_3} d\vec{q} \cdot \vec{\rho}(\vec{q}) \right] \\ &= \frac{2\pi}{3} W_{\mu_1-\mu_3}(\mathcal{S}_{C_{3,A}}) - \frac{1}{3} \int_{\mu_1-\mu_3} d\vec{q} \cdot \vec{\rho}(\vec{q}) = i \log \xi_{C_{3,A}} - \frac{1}{3} \int_{\mu_1-\mu_3} d\vec{q} \cdot \vec{\rho}(\vec{q}) \end{aligned} \quad (12)$$

Next, let us turn to the expression for γ_1 , Eq. (11) derived in Sec. D:

$$\gamma_1 = \gamma_1(\pi) + \frac{1}{2\pi} \int_{-\pi}^{\pi} dq_1 \int_{-\pi}^{\pi} dq_2 \mathcal{F}_{1,2}(\vec{q}) q_2$$

To exploit the rotational symmetry, we will change the domain of integration in the second term. For this purpose we divide the domain $[-\pi, \pi] \times [-\pi, \pi]$ into five parts, see Fig. 4, labeled as I, II, III, IV , and V , i.e.

$$BZ := [-\pi, \pi] \times [-\pi, \pi] = I \cup II \cup III \cup IV \cup V.$$

We wish to express the integral over BZ as an integral over the symmetric domain \overline{BZ} , see Fig. 4, consisting of $\overline{I}, \overline{II}, \overline{III}, \overline{IV}$, and V , i.e.

$$\overline{BZ} := \overline{I} \cup \overline{II} \cup \overline{III} \cup \overline{IV} \cup V.$$

Using this notation, we can write

$$\gamma_1 = \gamma_1(\pi) + \frac{1}{2\pi} \int_{\overline{BZ}} d\vec{q} \mathcal{F}_{1,2}(\vec{q}) q_2 + \int_{\overline{II-IV}} d\vec{q} \mathcal{F}_{1,2}(\vec{q}) = \gamma_{\mu_1} + \frac{1}{2\pi} \int_{\overline{BZ}} d\vec{q} \mathcal{F}_{1,2}(\vec{q}) q_2. \quad (13)$$

In the second equality we have employed Stokes' theorem. To make further progress, we need to specify the integration bounds explicitly. Here, we use the following parametrization:

$$\int_{\overline{BZ}} dq_1 dq_2 = \int_{-4\pi/3}^{4\pi/3} dq_1 \int_{b^-(q_1)}^{b^+(q_1)} dq_2,$$

with $b^+(q_1)$ given by

$$b^+(q_1) = \begin{cases} 2q_1 + 2\pi & \text{if } -\frac{4\pi}{3} \leq q_1 \leq -\frac{2\pi}{3} \\ \frac{1}{2}q_1 + \pi & \text{if } -\frac{2\pi}{3} \leq q_1 \leq \frac{2\pi}{3} \\ -q_1 + 2\pi & \text{if } \frac{2\pi}{3} \leq q_1 \leq \frac{4\pi}{3} \end{cases}$$

and $b^-(q_1)$ given by

$$b^-(q_1) = \begin{cases} -q_1 - 2\pi & \text{if } -\frac{4\pi}{3} \leq q_1 \leq -\frac{2\pi}{3} \\ \frac{1}{2}q_1 - \pi & \text{if } -\frac{2\pi}{3} \leq q_1 \leq \frac{2\pi}{3} \\ 2q_1 - 2\pi & \text{if } \frac{2\pi}{3} \leq q_1 \leq \frac{4\pi}{3} \end{cases}$$

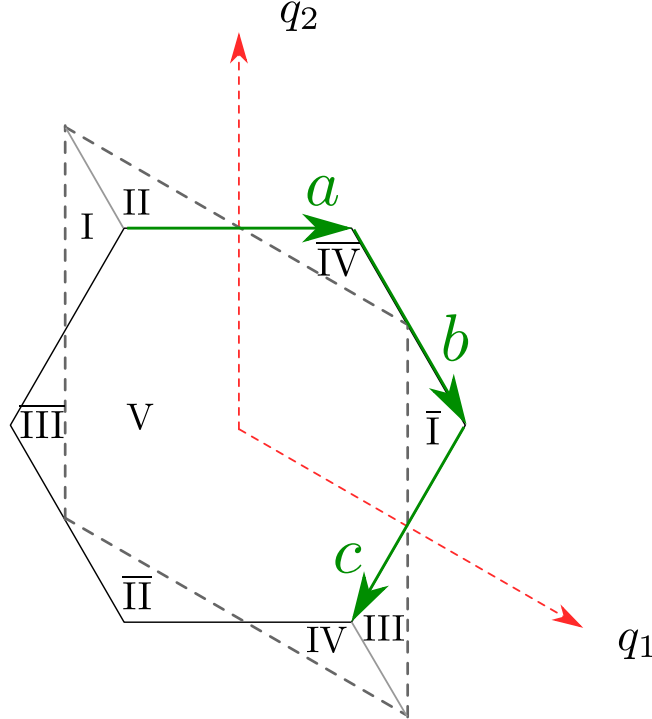


FIG. 4: The dashed lines enclose the domain $BZ = [-\pi, \pi] \times [-\pi, \pi]$. The green arrows denote the contours a , b , and c .

Note that b^+ is related to b^- in the following way

$$b^+(q_1) = \begin{cases} b^-(q_1 + 2\pi) & \text{if } -\frac{4\pi}{3} \leq q_1 \leq -\frac{2\pi}{3} \\ b^-(q_1) + 2\pi & \text{if } -\frac{2\pi}{3} \leq q_1 \leq \frac{2\pi}{3} \\ b^-(q_1 - 2\pi) + 2\pi & \text{if } \frac{2\pi}{3} \leq q_1 \leq \frac{4\pi}{3} \end{cases} \quad (14)$$

With the help of Eq. (10), we can express the second term in Eq. (13) as

$$\begin{aligned} \int_{\overline{BZ}} \mathcal{F}_{1,2}(\vec{q}) q_2 &= \frac{1}{3} \int_{\overline{BZ}} dq [\mathcal{F}_{1,2}(\vec{q}) + \mathcal{F}_{1,2}(R\vec{q}) + \mathcal{F}_{1,2}(R^2\vec{q})] q_2 - \frac{1}{3} \int dq_1 \int dq_2 (\partial_{q_1} \rho_2(\vec{q}) - \partial_{q_2} \rho_1(\vec{q})) q_2 \\ &\quad - \frac{1}{3} \int dq_1 \int dq_2 (-\partial_{q_2} \rho_2(\vec{q}) - \partial_{q_1} \rho_1(\vec{q}) - \partial_{q_2} \rho_1(\vec{q})) q_2 \\ &= \underbrace{-\frac{1}{3} \int_{-4\pi/3}^{4\pi/3} dq_1 \int_{b^-(q_1)}^{b^+(q_1)} dq_2 [\partial_{q_1} \rho_2(\vec{q})] q_2}_{(15)a} + \underbrace{\frac{2}{3} \int_{-4\pi/3}^{4\pi/3} dq_1 \int_{b^-(q_1)}^{b^+(q_1)} dq_2 [\partial_{q_2} \rho_1(\vec{q})] q_2}_{(15)b} \\ &\quad + \underbrace{\frac{1}{3} \int_{-4\pi/3}^{4\pi/3} dq_1 \int_{b^-(q_1)}^{b^+(q_1)} dq_2 [\partial_{q_1} \rho_1(\vec{q})] q_2}_{(15)c} + \underbrace{\frac{1}{3} \int dq_1 \int dq_2 [\partial_{q_2} \rho_2(\vec{q})] q_2}_{(15)d} \end{aligned} \quad (15)$$

Let us now work out the terms on the RHS of the equation above. Let us start with the first term. We move the derivative in front of the integral over q_2 :

$$\begin{aligned} (15)a &= -\frac{1}{3} \int_{-4\pi/3}^{4\pi/3} dq_1 \partial_{q_1} \int_{b^-(q_1)}^{b^+(q_1)} dq_2 \rho_2(\vec{q}) q_2 + \frac{1}{3} \int_{-4\pi/3}^{4\pi/3} dq_1 b^+(q_1) \rho_2(q_1, b^+(q_1)) \partial_{q_1} b^+(q_1) \\ &\quad - \frac{1}{3} \int_{-4\pi/3}^{4\pi/3} dq_1 b^-(q_1) \rho_2(q_1, b^-(q_1)) \partial_{q_1} b^-(q_1) \end{aligned}$$

The first term on the RHS vanishes because $b^+(\pm 4\pi/3) = b^-(\pm 4\pi/3)$. With the help of Eq. (14), we can combine the second and third term:

$$\frac{1}{6} \int_{-2\pi/3}^{2\pi/3} dq_1 \rho_2(q_1, b^+(q_1)) \cdot 2\pi + \frac{2}{3} \int_{-4\pi/3}^{-2\pi/3} dq_1 \rho_2(q_1, b^+(q_1)) \cdot 0 - \frac{1}{3} \int_{2\pi/3}^{4\pi/3} dq_1 \rho_2(q_1, b^+(q_1)) \cdot 2\pi = 0.$$

In the equation above the first and third term cancel against each other. Next, we consider the second term on the RHS of Eq. (15). Upon integration by parts, we find

$$\begin{aligned} (15)b &= -\frac{2}{3} \int dq_1 \int dq_2 \rho_1(\vec{q}) + \frac{2}{3} \int_{-4\pi/3}^{4\pi/3} dq_1 [b^+(q_1) \rho_1(q_1, b^+(q_1)) - b^-(q_1) \rho_1(q_1, b^-(q_1))] \\ &= -\frac{2}{3} \int dq_1 \int dq_2 \rho_1(\vec{q}) + \frac{4\pi}{3} \int_{-2\pi/3}^{4\pi/3} dq_1 \rho_1(q_1, b^+(q_1)) = -\frac{8\pi^2}{3} \rho_1 + \frac{4\pi}{3} \int_{-2\pi/3}^{4\pi/3} dq_1 \rho_1(q_1, b^+(q_1)). \end{aligned}$$

The third term vanishes for the same reason as the first term:

$$\begin{aligned} (15)c &= \frac{1}{3} \int_{-4\pi/3}^{4\pi/3} dq_1 \partial_{q_1} \int_{b^-(q_1)}^{b^+(q_1)} dq_2 \rho_1(\vec{q}) q_2 \\ &\quad - \frac{1}{3} \int_{-4\pi/3}^{4\pi/3} dq_1 [b^+(q_1) \partial_{q_1} b^+(q_1) \rho_1(q_1, b^+(q_1)) - b^-(q_1) \partial_{q_1} b^-(q_1) \rho_1(q_1, b^-(q_1))] \\ &= 0 \end{aligned}$$

Finally, let us rewrite the fourth term:

$$\begin{aligned} (15)d &= -\frac{1}{3} \int dq_1 \int dq_2 \rho_2(\vec{q}) + \frac{1}{3} \int_{-4\pi/3}^{4\pi/3} dq_1 [b^+(q_1) \rho_2(q_1, b^+(q_1)) - b^-(q_1) \rho_2(q_1, b^-(q_1))] \\ &= -\frac{1}{3} \int dq_1 \int dq_2 \rho_2(\vec{q}) + \frac{2\pi}{3} \int_{-2\pi/3}^{4\pi/3} dq_1 \rho_2(q_1, b^+(q_1)) = -\frac{4\pi^2}{3} \rho_2 + \frac{2\pi}{3} \int_{-2\pi/3}^{4\pi/3} dq_1 \rho_2(q_1, b^+(q_1)) \end{aligned}$$

Hence, if we now combine Eqs. (12), (13), and (15) we find

$$\begin{aligned}\gamma_1 &= i \log \xi_{C_{3,A}} - \frac{1}{3} \int_{\mu_1 - \mu_3} d\vec{q} \cdot \vec{\rho}(\vec{q}) - \frac{4\pi}{3} \rho_1 - \frac{2\pi}{3} \rho_2 + \frac{1}{3} \int_{-2\pi/3}^{4\pi/3} dq_1 \rho_2(q_1, b^+(q_1)) + \frac{2}{3} \int_{-2\pi/3}^{4\pi/3} dq_1 \rho_1(q_1, b^+(q_1)) \\ &= i \log \xi_{C_{3,A}} - \frac{4\pi}{3} \rho_1 - \frac{2\pi}{3} \rho_2 = i \log \xi_{C_{3,A}} - \frac{2\pi}{3} \rho_B + \frac{2\pi}{3} \rho_C\end{aligned}$$

Here, we have used that the second term cancels the last two integrals. Following the same steps for γ_2 , we obtain

$$\gamma_2 = i \log \xi_{C_{3,A}} + \frac{2\pi}{3} \rho_1 - \frac{2\pi}{3} \rho_2 = i \log \xi_{C_{3,A}} - \frac{2\pi}{3} \rho_B - \frac{4\pi}{3} \rho_C$$

Derivation of Eq. (6)

First, let us relate the partial Berry phase along the contour μ_1 to the \mathbb{Z}_3 -invariant $\chi_{C_{3,A}}$. For the purpose of the proof, we assume that we have found a time-reversal symmetric gauge along the contours μ_i . Then we can write

$$\begin{aligned}\gamma_{\mu_{i+1}}^I &= \int_{\mu_i^{1/2}} dR\vec{q} \cdot \text{Tr}[\mathcal{A}(R\vec{q})] = \int_{\mu_i^{1/2}} d\vec{q} \cdot \text{Tr}[\mathcal{A}(\vec{q})] + i \int_{\mu_i^{1/2}} d\vec{q} \cdot \nabla_{\vec{q}} \log \det \mathcal{S}_{\vec{C}_{3,A}}^{\dagger}(\vec{q}) + \int_{\mu_i^{1/2}} d\vec{q} \cdot \vec{\rho}(\vec{q}) \\ &= \gamma_{\mu_i}^I - 2\pi W_{\mu_i}^{1/2}(\mathcal{S}_{\vec{R}_A}) + \int_{\mu_i^{1/2}} d\vec{q} \cdot \vec{\rho}(\vec{q}).\end{aligned}$$

This implies:

$$\begin{aligned}\gamma_{\mu_1}^I &= \frac{2\pi}{3} W_{\mu_1 - \mu_3}^{1/2}(\mathcal{S}_{\vec{R}_A}) - \frac{1}{3} \int_{\mu_1^{1/2} - \mu_3^{1/2}} d\vec{q} \cdot \vec{\rho}(\vec{q}) = i \log \chi_{C_{3,A}} - \frac{1}{3} \int_{\mu_1^{1/2} - \mu_3^{1/2}} d\vec{q} \cdot \vec{\rho}(\vec{q}) \\ &= i \log \chi_{C_{3,A}} - \frac{1}{6} \int_{\mu_1 - \mu_3} d\vec{q} \cdot \vec{\rho}(\vec{q})\end{aligned}\tag{16}$$

Now, let us consider γ_1^I . First, we express γ_1^I as an integral over the rotation-symmetric domain \overline{BZ}

$$\begin{aligned}\gamma_1^I &= \gamma_1^I(\pi) + \frac{1}{4\pi} \int_{-\pi}^{\pi} dq_1 \int_{-\pi}^{\pi} dq_2 \mathcal{F}_{1,2}(\vec{q}) q_2 = \gamma_1^I(\pi) + \frac{1}{2} \int_{\overline{IV}} d\vec{q} \mathcal{F}_{1,2}(\vec{q}) + \frac{1}{4\pi} \int_{\overline{BZ}} d\vec{q} \mathcal{F}_{1,2}(\vec{q}) q_2 \\ &= \gamma_1^I(\pi) + \int_{\overline{IV}} d\vec{q} \mathcal{F}_{1,2}(\vec{q}) + \frac{1}{4\pi} \int_{\overline{BZ}} d\vec{q} \mathcal{F}_{1,2}(\vec{q}) q_2 = \gamma_{\mu_1}^I + \frac{1}{4\pi} \int_{\overline{BZ}} d\vec{q} \mathcal{F}_{1,2}(\vec{q}) q_2.\end{aligned}$$

In the third equality we have used that $\mathcal{F}_{1,2}(\vec{q}) = -\mathcal{F}_{1,2}(-\vec{q})$, and in the fourth equality we have employed Stokes theorem. Using Eqs. (15) and (16) we finally obtain

$$\gamma_1^I = i \log(\chi_{C_{3,A}}) - \frac{\pi}{3} \rho_B + \frac{\pi}{3} \rho_C$$

In a similar fashion we find

$$\gamma_2^I = i \log(\chi_{C_{3,A}}) - \frac{\pi}{3} \rho_B - \frac{2\pi}{3} \rho_C.$$

Spin-orbit coupling Hamiltonians

Here, we give the SOC Hamiltonians that we have used for the honeycomb lattice. The Rashba SOC Hamiltonian reads:

$$\tilde{H}_{\text{RSO}}(\vec{q}) = i\lambda_{\text{RSO}} \begin{pmatrix} 0 & 1 \\ -1 & 0 \end{pmatrix} \otimes \left(\frac{\sqrt{3}}{2} \sigma_2 + \frac{1}{2} \sigma_1 \right) + i\lambda_{\text{RSO}} \begin{pmatrix} 0 & e^{-iq_1} \\ -e^{iq_1} & 0 \end{pmatrix} \otimes \left(-\frac{\sqrt{3}}{2} \sigma_2 + \frac{1}{2} \sigma_1 \right) - i\lambda_{\text{RSO}} \begin{pmatrix} 0 & e^{-iq_2} \\ -e^{iq_2} & 0 \end{pmatrix} \otimes \sigma_1,$$

and

$$\tilde{H}_{\text{ISO}}(\vec{q}) = \lambda_{\text{ISO}} f(\vec{q}) \begin{pmatrix} 1 & 0 \\ 0 & -1 \end{pmatrix} \otimes \sigma_3.$$